ENCIT 2018

ABCM Associação Brasileira de Engenharia e Ciências Mecânicas

17th Brazilian Congress of Thermal Sciences and Engineering
November 25th-28th, 2018, Águas de Lindóia, SP, Brazil

ENCIT-2018-0087
EXPERIMENTAL INVESTIGATION OF LIQUID-SOLID FLUIDIZED BEDS IN A NARROW TUBE

Fernando David Cúñez Benalcázar
Erick de Moraes Franklin
University of Campinas, School of Mechanical Engineering, Rua Mendeleyev, 200, Campinas, 13083-860, Brazil
fernandodcb@fem.unicamp.br, franklin@fem.unicamp.br

Abstract. *The behavior of liquid-solid fluidized beds in a narrow tube is experimentally investigated. The fluidized beds are formed in a 25.4 mm-ID tube and consisted of alumina spheres with 6mm diameter and specific gravity of 3.69; So, the ratio between the spheres and the tube is 4.23. The experiments have been carried out with two water flow rates corresponding to mean cross-sectional velocities of* $\overline{U}$ *= 0.137 and 0.164m/s, and three different arrangements of beds with 250, 400 and 500 spheres were used. With these conditions, it was possible to observe the formation of transverse waves, in the form of granular plugs that propagate with characteristic lengths and celerities. The fluidized beds were filmed with a high-speed camera, and the images were processed by using numerical codes in order to automatically identify and track the plugs.*

Keywords: *fluidized bed, liquid-solid, narrow tube, transverse waves.*

1. INTRODUCTION

A fluidized bed is a suspension of solid particles (grains) in a vertical tube submitted to an ascendant fluid flow. Given their high heat and mass transfers, fluidized beds are frequently employed in oil and coal industrial processes such as combustion or gasification of coal or biomass, and drying, cooling and coating of solids. In fact, with the growing importance of fossil energy, fluidized beds were used more extensively at the beginning of the 20th century (Nicolas *et al.*, 1999; Guazzelli, 2005). In the 21th century, the increasing use of solid biomass materials has revived our interest in the use of fluidized beds. Uniform fluidized beds are uncommon in industrial facilities, and usually instabilities appear. These instabilities consist of transverse waves, bubbles, or long bubbles.

Over the past decades, many papers investigated the flow regimes in liquid-solid fluidized beds (Nicolas *et al.*, 1999; Anderson and Jackson, 1968, 1969; El-Kaissy and Homsy, 1976; Didwania and Homsy, 1981; Zenit *et al.*, 1997; Zenit and Hunt, 2000; Duru and Guazzelli, 2002; Duru *et al.*, 2002; Aguilar-Corona *et al.*, 2011; Ghatage *et al.*, 2014). Some of them were interested in fluidized beds in narrow ducts of rectangular cross section (El-Kaissy and Homsy, 1976; Didwania and Homsy, 1981; Duru and Guazzelli, 2002), where the thickness is between 10 to 100 grain diameters, and some few papers investigated liquid-solid fluidized beds in narrow pipes (Anderson and Jackson, 1969; Zenit *et al.*, 1997; Zenit and Hunt, 2000; Duru *et al.*, 2002; Aguilar-Corona *et al.*, 2011; Ghatage *et al.*, 2014). Although there is not a consensus about it, we consider in this paper that for a narrow pipe the ratio between the tube and grain diameters is less than approximately 50. For liquid-solid fluidized beds in narrow tubes, the dynamics and instabilities are different due to high confinement effects; therefore, this case is still to be understood.

In this paper we investigate one pattern appearing in beds fluidized by water in a very narrow tube. Confinement effects caused by the narrow tube combined with the lubrication and virtual mass forces, which are significant under water, are the origin of alternating high- and low-compactness regions, known as plugs and bubbles, respectively. Although this instability is present in industrial applications, there have been very few studies about it, and its dynamics is still to be understood. Few previous experimental studies were made to understand the problem, without exhausting it, and, to the authors' knowledge, no one investigated the very narrow case for which the ratio between the tube and grain diameters is between 2 and 5. The objective of this study is to obtain experimentally the lengths and celerities of granular plugs in very narrow tubes. The experimental results are presented for the first time in this paper.

The fluidized beds were formed in a 25.4 mm-ID tube and consisted of alumina spheres with 6 mm diameter and specific density of 3.69. The ratio between the tube and grain diameters was 4.23; therefore, we consider the tube as a very narrow one. For the experiments, we filmed the fluidized bed with a high-speed camera, and automatically identified and tracked the plugs along images by using numerical scripts.

2. EXPERIMENTAL SETUP

The schematic of the experimental apparatus is depicted in Fig.1. The experimental setup consisted of a water reservoir, a heat exchanger, a centrifugal pump, a flow meter, a flow homogenizer, a 25.4 mm-ID tube with vertical and horizontal sections, and a return line. So, the water flowed in a closed loop in the order described above.

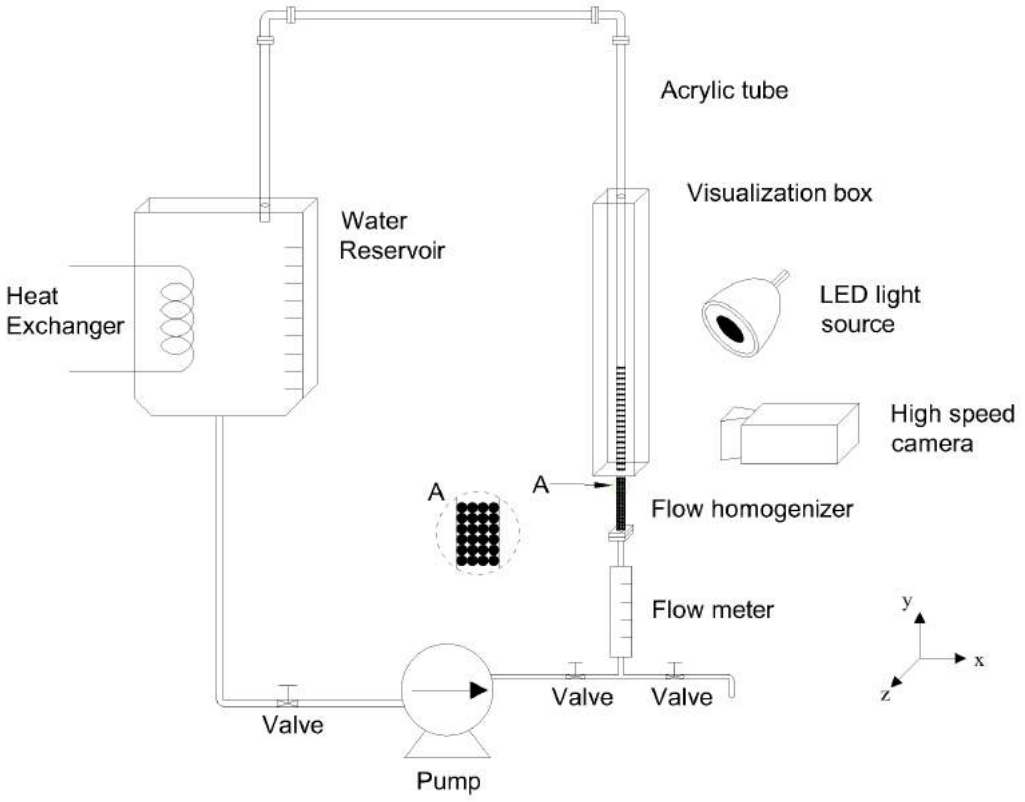

Figure 1. Layout of the experimental setup.

The vertical section was a 1.2 m-long, 25.4 mm-ID transparent PMMA (Polymethyl methacrylate) tube, of which 0.65 m was the test section. The vertical tube was vertically aligned within $\pm 3°$. A visualization box filled with water was mounted in the test section to ensure proper photographic images. A flow homogenizer consisting of a fixed bed of packed alumina spheres with $d = 6$ mm was used to provide uniform water flows at the inlet of the test section. The water temperature was maintained at 25°C $\pm$ 3°C by a heat exchanger mounted in the water reservoir. The water flow rates were adjusted with a set of globe valves.

Three different arrangements of beds with 250, 400 and 500 spheres with mean diameter of 6 $\pm$ 0.03 mm and S = ρ_p/ρ_f = 3.69, where ρ_p is the density of the bead material and ρ_f the density of the fluid, were used as solid fluidized particles. The Stokes and Reynolds numbers based on terminal velocities were $St_t = v_t d\rho_p/(9\mu_f)$ = 1650 and $Re_t = \rho_f v_t d/\mu_f$ = 4026, respectively, where v_t is the terminal velocity of one single particle and μ_f is the dynamic viscosity of the fluid. The bed heights at the inception of fluidization h_{mf} were in average 117, 181 and 225 mm for the beds consisting of 250, 400 and 500 particles, respectively, from which the liquid volume fraction at the inception of fluidization ε_{mf} was computed. The settling velocity at the inception of fluidization, computed based on the Richardson–Zaki correlation, was $v_s = v_t \varepsilon_{mf}^{2.4}$ = 0.13 m/s. Two water flow rates were imposed, Q = 250 l/h and Q = 300 l/h, for which the corresponding superficial velocities $\overline{U} = 4Q/\pi D^2$, fluid velocities trough the packed bed $U_f = \overline{U}/\varepsilon_{mf}$, Reynolds numbers based on the tube diameter $Re_D = \rho_f \overline{U} D/\mu_f$, and Reynolds numbers based on the grain diameter $Re_d = \rho_f \overline{U} d/\mu_f$ are summarized in Tab. 1.

The liquid-solid fluidized beds were filmed with a high-speed camera of CMOS (Complementary Metal Oxide Semiconductor) type having a resolution of 1600 $px \times 2560$ px at frequencies up to 1400 Hz at full resolution. To provide the necessary light for low exposure times while avoiding beating between the light source and the camera frequency, LED (Low Emission Diode) lamps were branched to a continuous current source. In this study, the camera frequency was set to between 100 Hz and 200 Hz. The number of acquired images for each test was 5000 and the total number of tests was 6, giving a total of 30000 images to be analyzed. MATLAB scripts were written in order to process the obtained images.

Table 1. Grain diameter d, terminal Reynolds number Re_t, terminal Stokes number St_t, water flow rate Q, superficial velocity $\overline{U}$, Reynolds number based on the tube diameter Re_D, Reynolds number based on the grain diameter $Re_d = \rho_f \overline{U} d/\mu_f$, settling velocity v_s, and fluid velocities trough the packed bed U_f.

d mm	Re_t $\cdots$	St_t $\cdots$	Q l/h	$\overline{U}$ m/s	Re_D $\cdots$	Re_d $\cdots$	v_s m/s	U_f m/s
6	4026	1650	250	0.137	3481	822	0.13	0.27
6	4026	1650	300	0.164	4177	987	0.13	0.32

3. RESULTS

Under the tested conditions, granular plugs and liquid bubbles (void regions) occupying the entire tube cross section were observed in the fluidized bed. Those forms, that were nearly one dimensional, propagated upwards with characteristic lengths and celerities.

Figures 2 and 3 present some frames obtained with the high-speed camera for the 250, 400 and 500 particles beds for both flow rates, respectively. The corresponding times are in the caption of figures. From these figures, we can observe the plugs and bubbles in the bed.

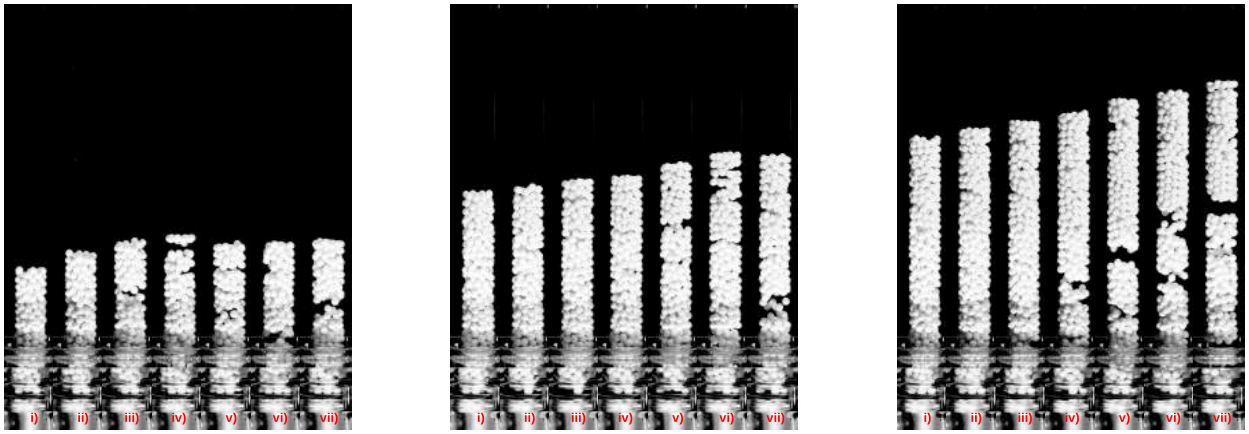

(a) (b) (c)

Figure 2. Instantaneous snapshots of particles positions: (a) N = 250 and $\overline{U}$ = 0.137 m/s; (b) N = 400 and $\overline{U}$ = 0.137 m/s; (c) N = 500 and $\overline{U}$ = 0.137 m/s. The corresponding times are: (i) 0 s; (ii) 1 s; (iii) 1.5 s; (iv) 2 s; (v) 2.5 s; (vi) 3 s; (vii) 3.5 s.

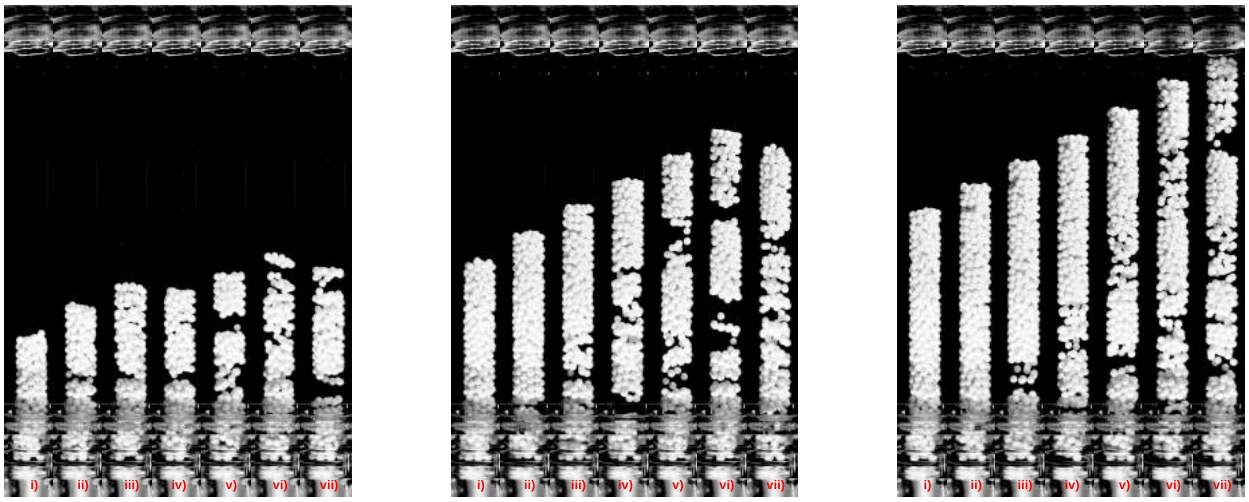

(a) (b) (c)

Figure 3. Instantaneous snapshots of particles positions: (a) N = 250 and $\overline{U}$ = 0.164 m/s; (b) N = 400 and $\overline{U}$ = 0.164 m/s; (c) N = 500 and $\overline{U}$ = 0.164 m/s. The corresponding times are: (i) 0 s; (ii) 1 s; (iii) 1.5 s; (iv) 2 s; (v) 2.5 s; (vi) 3 s; (vii) 3.5 s.

The upward propagation of the void regions made the top of the bed oscillate between minimum and maximum values. Because of this oscillation, we computed the average height of the fluidized bed h_{avg} as the average between minimum and maximum values. In addition, we computed the upward, C_{up}, and downward, C_{down}, celerities of the top as the derivative of the measured positions during its rise and descent, respectively.

We identified and followed each granular plug in the high-speed movies by using numerical scripts whose description can be found in Alvarez and Franklin (2017). We present next the length scales and the celerities obtained from the experiments. Table 2 presents the superficial velocity $\overline{U}$, number of grains N, initial bed height h_{mf}, length scale of plugs λ, standard deviation of length scale σ_λ, length scale of plugs normalized by the grain diameter λ/d, standard deviation of length scale normalized by the grain diameter σ_λ/d, bed upward celerity C_{up}, standard deviation of upward celerities $\sigma_{C,up}$, bed downward celerity C_{down}, standard deviation of downward celerities $\sigma_{C,down}$, and average height of the fluidized bed h_{avg}.

Table 2. Superficial velocity $\overline{U}$, Number of grains N, initial bed height h_{mf}, length scale of plugs λ, standard deviation of length scale σ_λ, length scale of plugs normalized by the grain diameter λ/d, standard deviation of length scale normalized by the grain diameter σ_λ/d, bed upward celerity C_{up}, standard deviation of upward celerities $\sigma_{C,up}$, bed downward celerity C_{down}, standard deviation of downward celerities $\sigma_{C,down}$, and average height of the fluidized bed h_{avg}, obtained from experiments.

case	$\cdots$	(a)	(b)	(c)	(d)	(e)	(f)
$\overline{U}$	m/s	0.137	0.137	0.137	0.164	0.164	0.164
N	$\cdots$	250	400	500	250	400	500
h_{mf}	m	0.117	0.181	0.225	0.117	0.181	0.225
λ	m	0.075	0.082	0.072	0.040	0.041	0.042
σ_λ	m	0.027	0.047	0.046	0.026	0.028	0.030
λ/d	$\cdots$	12.4	13.7	11.9	6.6	6.8	7.1
σ_λ/d	$\cdots$	4.4	7.9	7.6	4.3	4.6	5.0
C_{up}	m/s	0.012	0.017	0.018	0.029	0.035	0.060
$\sigma_{C,up}$	m/s	0.007	0.009	0.008	0.016	0.017	0.061
C_{down}	m/s	-0.019	-0.029	-0.040	-0.049	-0.057	-0.114
$\sigma_{C,down}$	m/s	0.017	0.028	0.049	0.038	0.046	0.099
h_{avg}	m	0.142	0.226	0.287	0.177	0.287	0.354

Within the experimental conditions, the lengths of plugs show strong variations with the water flow and are independent of the initial height of the bed (or of the number of beads), despite the small variation in water superficial velocities (of only 20 %) when compared to the variation in the number of particles (of 100 %). The lengths of plugs were around $12d$ for $\overline{U}$ = 0.137 m/s and $7d$ for $\overline{U}$ = 0.164 m/s. This represents a variation of 100 % in λ for variations of 20 % in $\overline{U}$. Standard deviations of plug lengths are large. The reason for that is the discrete nature of plugs, which consist of solid particles that are large with respect to the plugs: the grain diameter is around 10 % of the plug length and 25 % of the tube diameter.

Bed celerities present variations with both the initial bed height and flow conditions. From N = 250 to N = 500, C_{up} varies from 0.012 to 0.018 m/s for $\overline{U}$ = 0.137 m/s and from 0.029 to 0.069 m/s for $\overline{U}$ = 0.164 m/s, while C_{down} varies from -0.019 to -0.040 m/s for $\overline{U}$ = 0.137 m/s and from -0.049 to -0.114 m/s for $\overline{U}$ = 0.164 m/s. This represents variations of 130 % in C_{up} and C_{down} for variations of 100 % in N, and of 230 % in C_{up} and 190 % in C_{down} for variations of 20 % in $\overline{U}$. As for λ, standard deviations of the celerities are large due to the relatively large size of solid particles.

In order to understand the distribution of the lengths of plugs along the tube, we computed the probability density functions (PDF) of the lengths of plugs normalized by the grain diameter d for both water flow rates. Figure 4 a) shows the probability density function of the lengths of the plugs for the three arrangements of beds and $\overline{U}$ = 0.137 m/s. From this figure, we can observe for N = 250, the distribution of the plugs lengths presents a different behavior when compared to the other two arrangements. For N =250 the lengths of plugs are around $15d$ with a little deviation, while for N = 400 and N = 500, the lengths of plugs are around $14d$ with a large deviation. This behavior is also observed in table 2, when the values of λ/d and σ_λ/d are compared. Figure 4 b) shows the probability density function of the lengths of the plugs for the three arrangements of beds and $\overline{U}$ = 0.164 m/s. From this figure, we can observe the distribution of the plugs lengths presents the same behavior for the three arrangements, where the lengths of the plugs are around $5d$.

For the first flow rate, the superficial velocity $\overline{U}$ is slightly higher than the settling velocity v_s, i.e., the flow rate is closer to minimum fluidization; therefore, with a small amount of spheres as the case of N = 250, the formation of only two plugs is expected, as observed in Fig. 2 a), and this could be the explanation for the behavior of the Fig.4 a).

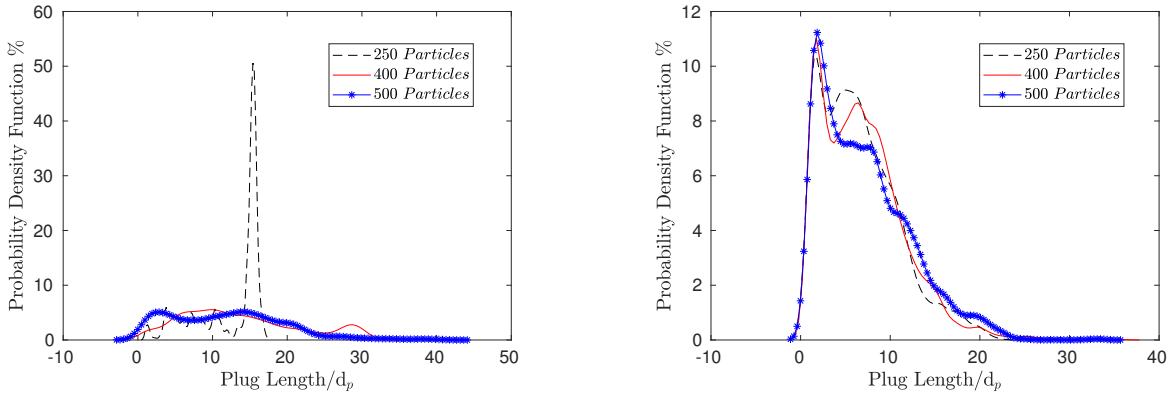

Figure 4. Probability density function of lengths of the plugs for the three arrangements of beds: (a) $\overline{U}$ = 0.137 m/s; (b) $\overline{U}$ = 0.164 m/s.

4. CONCLUSIONS

This paper investigated experimentally the dynamics of granular plugs in water fluidized beds in a very narrow tube. The confinement created by the narrow tube together with the lubrication and virtual mass forces lead to the formation of alternating high- and low-compactness regions, known as plugs and bubbles, which have characteristic lengths and celerities. Although this pattern is present in industrial applications, few previous studies were made to understand the problem, without exhausting it.

In the present study, fluidized beds were formed in a 25.4 mm-ID tube and consisted of alumina beads with 6 mm diameter and specific density of 3.69 fluidized by water flows. The ratio between the tube and grain diameters was 4.23, which is considered a very narrow case. In our experiments, the fluidized bed was filmed with a high-speed camera, and the plugs were automatically identified and tracked along images by using numerical scripts.

Under the experimental conditions, granular plugs and void regions occupying the entire tube cross section were observed in the fluidized bed. Despite the small variation in water superficial velocities when compared to the variation in the number of particles, the lengths of plugs strongly depended on the water flow and were independent of the initial height of the bed. Bed celerities showed variations with both the initial bed height and water flow.

We found from our experiments that the lengths of plugs were around $12d$ for $\overline{U}$ = 0.137 m/s and $7d$ for $\overline{U}$ = 0.164 m/s. The bed celerities in the upward direction varied between 0.012 and 0.060 m/s and in the downward direction between -0.019 and -0.114 m/s.

5. ACKNOWLEDGEMENTS

Fernando David Cúñez Benalcázar is grateful to FAPESP (grant no. 2016/18189-0), and Erick de Moraes Franklin would like to express his gratitude to FAPESP (grant no. 2016/13474-9) and CNPq (grant no. 400284/2016-2) for the financial support they provided.

6. REFERENCES

Aguilar-Corona, A., Zenit, R. and Masbernat, O., 2011. "Collisions in a liquid fluidized bed". *Int. J. Multiphase Flow*, Vol. 37, No. 7, pp. 695 – 705.

Alvarez, C.A. and Franklin, E.M., 2017. "Intermittent gravity-driven flow of grains through narrow pipes". *Physica A*, Vol. 465, pp. 725 – 741.

Anderson, T.B. and Jackson, R., 1968. "Fluid mechanical description of fluidized beds. Stability of the state of uniform fluidization". *Ind. Eng. Chem. Fundamen.*, Vol. 7, pp. 12–21.

Anderson, T.B. and Jackson, R., 1969. "A fluid mechanical description of fluidized beds. Comparison of theory and experiment". *Ind. Eng. Chem. Fundamen.*, Vol. 8, No. 1, pp. 137–144.

Didwania, A.K. and Homsy, G.M., 1981. "Flow regimes and flow transitions in liquid fluidized beds". *Int. J. Multiphase Flow*, Vol. 7, No. 6, pp. 563–580.

Duru, P. and Guazzelli, É., 2002. "Experimental investigation on the secondary instability of liquid-fluidized beds and the formation of bubbles". *J. Fluid Mech.*, Vol. 470, pp. 359–382.

Duru, P., Nicolas, M., Hinch, J. and Guazzelli, É., 2002. "Constitutive laws in liquid-fluidized beds". *J. Fluid Mech.*, Vol. 452, pp. 371–404.

El-Kaissy, M.M. and Homsy, G.M., 1976. "Instability waves and the origin of bubbles in fluidized beds: Part 1: Experiments". *Int. J. Multiphase Flow*, Vol. 2, No. 4, pp. 379 – 395.

Ghatage, S.V., Peng, Z., Sathe, M.J., Doroodchi, E., Padhiyar, N., Moghtaderi, B., Joshi, J.B. and Evans, G.M., 2014. "Stability analysis in solid-liquid fluidized beds: Experimental and computational". *Chem. Eng. J.*, Vol. 256, pp. 169 – 186.

Guazzelli, É., 2005. *Fluidized beds: from waves to bubbles*, Wiley-VCH Verlag GmbH & Co. KGaA, chapter 9, pp. 211–232.

Nicolas, M., Hinch, J. and Guazzelli, É., 1999. "Wavy instability in liquid-fluidized beds". *Ind. Eng. Chem. Res.*, Vol. 38, No. 3, pp. 799–802.

Zenit, R. and Hunt, M.L., 2000. "Solid fraction fluctuations in solid-liquid flows". *Int. J. Multiphase Flow*, Vol. 26, No. 5, pp. 763 – 781.

Zenit, R., Hunt, M.L. and Brennen, C.E., 1997. "Collisional particle pressure measurements in solid-liquid flows". *J. Fluid Mech.*, Vol. 353, pp. 261–283.

7. RESPONSIBILITY NOTICE

The following text, properly adapted to the number of authors, must be included in the last section of the paper: The authors are the only responsible for the printed material included in this paper.